CO₂ Exchanges within Zones of Rapid Conversion from Permafrost Plateau to Bog and Fen Land Cover Types

L. Chasmer*†

A. Kenward*

W. Quinton* and

R. Petrone*

*Cold Regions Research Centre, Wilfrid Laurier University, 75 University Avenue West, Waterloo, Ontario, N2L 3C5, Canada
†Corresponding author: laura.chasmer@gmail.com

Abstract

Variability of midday net ecosystem CO_2 exchange (NEE) and respiration was measured using a transect of closed system chambers spanning transitions from channel fen, permafrost plateau, and ombrotrophic flat bog land cover types during the spring melt season (26 April–6 June 2008). The primary objective was to compare fluxes from different land cover types and topographic variability within zones adjacent to and including rapid permafrost thaw. During this period, the bog was the greatest net source of CO_2 to the atmosphere, followed by plateau, and fen. NEE was slightly positive (indicating CO_2 loss to the atmosphere) during the snowmelt period (average = 0.009 ± 0.004 mg CO_2 m^{-2} s^{-1}), and increased to 0.025 ± 0.012 mg CO_2 m^{-2} s^{-1}, on average, possibly due to soil thaw and increased microbial activity within two days of completely snow-free conditions. Near surface soil temperature and depth to the water table were the most significant controls of soil and ground cover CO_2 fluxes within chambers at all sites ($p < 0.05$). Analysis of historical aerial photographs and satellite imagery of the area from 1947 to 2008 indicates that plateaus are converting more rapidly into bogs than fen, where 73% of plateau areas (since 1970) that thawed had become bogs (as opposed to 27% conversion into fen). Future research requires establishment of a full ecosystem or land cover greenhouse gas and soil nutrient exchange/transfer program, including CO_2 and water fluxes as well as dissolved organic and inorganic C, and CH_4 losses from the soil. These results contribute to a better understanding of northern soil and ground-cover carbon exchanges as greater areas of permafrost plateaus collapse and form bogs.

Introduction

The discontinuous permafrost zone of North America is expanding as a result of a northward shift of the southern boundary of continuous permafrost, while the overall area coverage and density of permafrost has been shrinking (e.g. Quinton et al., 2010; Chasmer et al., 2011a). Ansimov and Reneva (1996) predicted that permafrost area will reduce by 15%–30% by 2050 as a result of warming air temperatures. Because northern peatlands contain approximately one-third of the global carbon (C) pool, and almost half of the atmospheric C pool (Gorham, 1991), small changes to land surface morphology, hydrology, and vegetation communities could have significant cumulative impacts to northern C exchanges and global climate change (Camill et al., 2001).

Several studies predict that northern (boreal/tundra) ecosystems will become a stronger source of C with increased air temperatures (e.g. Oechel et al., 1994; Goulden et al., 1998), while others suggest the opposite (e.g. Oechel et al., 2000; Turetsky et al., 2002; Myers-Smith et al., 2007, 2008). These tend to follow two opposing thoughts: (a) higher air temperatures will increase rates of permafrost thaw. Improved soil drainage and aridity due to creation of drainage channels may increase rates of decomposition, which will provide feedback to the global climate system by increasing global atmospheric CO_2 concentrations and air temperatures (e.g. Gorham, 1991). (b) Changes in vegetation community composition could result in increased C sequestration over many years, which will exceed C released via soil decomposition (e.g. Turetsky et al., 2002). Observations have been made to support both hypotheses;

however, their relevance to climate change will depend on the spatial extent of these observations within highly heterogeneous ecosystems and feedbacks between local energy, water and nutrient flows, and vegetation succession (Petrone et al., 2011).

The discontinuous permafrost region of Canada is exceedingly complex. Interactions between soil moisture, vegetation functional type and succession, and microclimate are difficult to separate and often confound relationships with C fluxes. Slight changes to local hydrology and energy receipt vary biotic and abiotic controls on the net directionality of C fluxes from sink to net source and *vice versa* (Moore et al., 1998; Trumbore et al., 1999; Bubier et al., 2003; Sulman et al., 2010; Wilson and Humphreys, 2010; Humphreys and Lafleur, 2011). Generally, microtopographic highs (hummocks, etc.) are dryer than microtopographic lows (hollows, depressions, etc.) (Waddington and Roulet, 1996; Petrone et al., 2005), and these often contain different vegetation community distributions and variable CO_2 fluxes (e.g. Oechel et al., 1994; Goulden et al., 1998; Strack et al., 2006; Johansson et al., 2006; Petrone et al., 2011; Wilson and Humphreys, 2010). Within the fragmented discontinuous permafrost zone, the spatial variability of water storage and drainage is even more crucial because of preferential thaw and the obstruction and redirection of water from plateaus through channel fens and bogs (Quinton et al., 2010). On plateaus, excess water is shed to adjacent fens and bogs as subsurface flow over the relatively impermeable frost table (Quinton and Marsh, 1999), which descends through the active layer during thaw (Hayashi et al., 2007). This often creates wetter (not drier) peatlands as permafrost thaws, resulting in changes to plant communities (Camill, 1999).

Local increases in radiation loading in areas of reduced canopy cover (as a result of tree mortality due to soil saturation) create preferential thaw of the active layer, thaw depressions, and changes to local hydrology and plant functional types (Wright et al., 2009; Hayashi et al., 2007; Quinton et al., 2010; Chasmer et al., 2011b), thereby affecting the C balance (e.g. Myers-Smith et al., 2007).

Rates of C exchange within northern peatlands, including those underlain with permafrost support (a) soil drying, increased decomposition, increased CO_2 efflux; and (b) soil drying, changes to plant functional types, and increased CO_2 sequestration hypotheses, depending on local environmental/topographical conditions and land cover type. Goulden et al. (1998) found that respiration increased during warm summer months in a 120-year-old black spruce forest in northern Manitoba, while photosynthesis remained fairly constant. They suggested that the depth to the frost table and increasing volume of unfrozen soil throughout the summer had the greatest influence on CO_2 efflux, while saturated wetlands were not prone to seasonal increases in respiration due to anoxic soil conditions after thaw. During the winter to spring shoulder period, Bubier et al. (2002) found that the largest release of CO_2 occurred when ground temperatures reached 0 °C in a temperate peatland. Degassing of soils likely occurred as a result of the buildup and release of stored CO_2 as soon as the ground thawed, and also likely increased microbial activity. They note that emissions of between 3% and 50% of annual CO_2 efflux in northern ecosystems vary due to soil moisture status, the length of the nongrowing season, snow cover, and temperature. Further, increased CO_2 effluxes were also associated with deeper snow packs, likely as a result of soil insulation from freezing air temperatures and minimal microbial activity.

Vegetation succession and changes in plant functional type that occur as trends in local soil moisture change can also have significant influences on C fluxes. For example, Turetsky et al. (2000, 2002), found that wet internal lawns (depressions) had greater C uptake likely as a result of increased bryophyte primary production, while Petrone et al. (2011) found that *Sphagnum*-dominant lawns had greatest C uptake compared with feather moss-dominant lawns and *Sphagnum*- and feather moss-dominant depressions. Reduced overstory canopy cover and increased photosynthetically active radiation (PAR) incident on *Sphagnum*-dominant lawns increased photosynthesis. This is supported by greater maximum CO_2 assimilation (A_{max}) found for *Sphagnum*-dominant lawns compared with those of feather moss (Petrone et al., 2011). Within peatlands in northern England, Ward et al. (2009) found that changes to plant functional groups and composition affected short-term C fluxes, especially if rapid CO_2 uptake and turnover via graminoids is altered by the migration and growth of dwarf shrubs. These reduce CO_2 uptake because of shading by dwarf shrubs and litter accumulation. Artificial application of N to vegetation within plots also increased biomass and leaf area, but reduced net ecosystem exchanges (NEE) due to reduced moss photosynthesis (Bubier et al., 2007). Over longer time periods, Camill et al. (2001) found that changes in biomass and decomposition were more strongly related to vegetation succession than climatic changes within the discontinuous permafrost region of northern Manitoba. However, warmer air temperatures and predicted drought (due to increased evaporation and evapotranspiration in

these areas) are hypothesized to reduce the success of black spruce and *Sphagnum* vegetation communities, which could lead to decreases in the efficiency of ecosystem C storage over the long term (Myers-Smith et al., 2008). Further, because C accumulation is greater in areas of permafrost collapse (Myers-Smith et al., 2008), climate warming and forest fires (inducing further permafrost collapse) could result in greater C storage, while increased drying and decomposition will have the opposite effect (Camill and Clark, 1998; Robinson and Moore, 2000). Myers-Smith et al. (2007) suggested that expansion of peatland vegetation with warming air temperatures will likely result in increased C uptake, but also increased CH_4 emissions as permafrost degrades.

The sensitivity of permafrost degradation to increasing air temperatures and topographic morphology (as a mechanism for water movement and transfer of heat through the soil column) has been documented in several studies (e.g. Camill and Clark, 1998; Quinton et al., 2009), but has not been related to changes in C fluxes at the plateau/peatland margin where the greatest changes are taking place. In this study, we examine for the first time relationships between the 3D topographical characteristics of the land surface derived from very high resolution airborne Light Detection And Ranging (LiDAR), soil and ground cover CO_2 fluxes, and soil chemistry. The objectives of this study are to: (1) compare CO_2 fluxes within and between plateau, bog, and fen sites, which will provide evidence to support soil drying/efflux and/or vegetation succession/uptake hypotheses per land cover type; (2) quantify environmental influences on fluxes, including meteorological, microtopographic, and soil property; and (3) discuss possible implications of climate change in the discontinuous permafrost zone by quantifying plateau conversion to bogs and fens from historic aerial photography and satellite imagery. This study focuses on the critical final transition from the early snowmelt to snow-free period. This is the most hydrologically dynamic period in the discontinuous permafrost zone, initiating microbial activity, photosynthesis, and gas exchanges between the biosphere and the atmosphere (Griffis et al., 2000; Humphreys and Lafleur, 2011). Feedbacks and feedback strength related to land cover type, topography, and vegetation structure will be quantified.

Study Site

CO_2 exchange was measured within the Scotty Creek watershed (61°18′N, 121°18′W), 50 km south of Fort Simpson, Northwest Territories, Canada. An ~160-m-long transect was established through channel fen, permafrost plateau, and flat ombrotrophic bog land cover types (Fig. 1). The channel fen is located on the northwest side of the permafrost plateau and contains a ground cover of primarily *Carex* spp., *Helodium blandowii*, *Brachytheuum rivulane*, *Aulacommium palustre*, and patches of shrubs with some *Picea mariana* (Table 1; Hayashi et al., 2004). Soils are comprised of a dense organic layer with mineral soils extending to a depth of 3 m below the water surface (Hayashi et al., 2004). The permafrost plateau rises ~0.9 m above the surrounding peatlands and is rapidly degrading at an average rate of 0.3 m per year on the northwest side (from 1977 to 2008 determined from aerial photography; Chasmer et al., 2011a). Signs of ground surface collapse are evident along the outer perimeter of the plateau, with additional subsidence in areas of isolated surficial permafrost loss

Permafrost Plateau
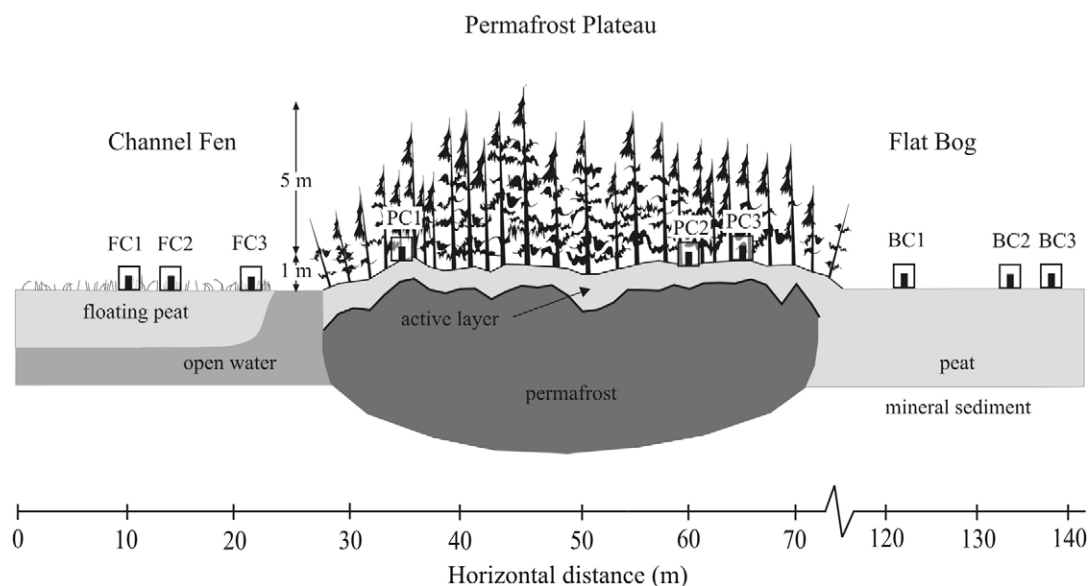
FIGURE 1. Schematic cross-section illustration of CO$_2$ flux chambers along an ~140 m transect traversing channel fen, permafrost plateau, and flat bog land cover types within the Scotty Creek watershed. Each chamber was located within representative topographically upraised, depression, and edge parts of land cover types. FC = Fen chamber 1, 2, and 3; PC = Plateau chamber 1, 2, and 3; and BC = Bog chamber 1, 2, and 3. Vegetation heights (fen and plateau) range between 1 m and 5 m in height (denoted by arrows) (After Quinton et al., 2011).

towards the center. The plateau supports an open tree canopy of *Picea mariana* with average canopy heights of 3.1 m (±2.2 m) and a density of 1 stem m^{-2} (Wright et al., 2008). Ground cover is mainly *Betula glandulosa*, *Rubus chamaemorus*, and *Sphagnum capilofolium* (Table 1). An organic peat layer extends to a depth of up to 8 m, under which a silt-sand layer and thick clay to silt-clay layer exists (Aylesworth and Kettles, 2000). The upper plateau soil layer (0.2–0.5 m) comprises living vegetation, and a newly

decomposed fibric peat layer, under which lies a layer of dense sylvic peat containing wood material, lichen, moss, rootlets, and needles at a more advanced state of decomposition (Quinton et al., 2003).

Peat deposit within bogs and fens in this region have an average thickness of 2.4 m and are underlain by a mineral silt-sand layer ranging in thickness up to 1 m. The mineral silt-sand layer overlays a thick layer (6 m on average) of glaciolacustrine clay

TABLE 1

Vegetation canopy characteristics (± range) within 2 m radius of center of chamber measurement location, and vegetation species types within chambers (only).

Chamber site (landcover type)	Canopy species	Understory species (% cover within chambers [averages])	Ground cover species (% cover within chambers [averages])
PC1 (Plateau)	*Picea mariana*	*Rubus chamaemorus* (2%), *Ledum groenlandicum* (5%), *Oxyoccus microcarpus* (5%), *Vaccinium vitis-idaea* (5%), *Betula glandulosa* (10%)	*Sphagnum capillifolium/fuscum* (90%), *Sphagnum girgensohnii* (10%)
PC2 (Plateau)	*Picea mariana*	*Rubus chamaemorus* (5–10%), *Oxyoccus microcarpus* (2%)	*Sphagnum capillifolium* (90%), *Sphagnum girgensohnii* (10%)
PC3 (Plateau)	*Picea mariana*	*Rubus chamaemorus*(10%), *Ledum groenlandicum* (2%)	*Cladina mitis, Cladina rangiferina* (85%); bare ground (15%)
BC1 (Bog)	No canopy	*Carex* spp. (2–5%), *Andromeda polifolia* (5%), *Chamaedaphne calyculata* (5%)	*Sphagnum capillifolium* (50%), *Sphagnum fuscum* (50%)
BC2 (Bog)	No canopy	*Carex* spp. (1%)	*Sphagnum capillifolium* (50%), *Sphagnum fuscum* (50%)
BC3 (Bog)	No canopy	*Carex* spp. (2%), *Chamaedaphne calyculata* (1%)	*Sphagnum capillifolium* (50%), *Sphagnum fuscum* (50%)
FC1 (Fen)	No canopy	*Oxyoccus microcarpus* (5%), *Potentilla palustris* (10%), *Salix pedicellaris* (10%), *Carex* spp. (15%)	*Helodium blandowii* (50%); *Sphagnum squarrosum, Brachythecium rivulare* (40%); *Aulacomnium palustre* (10%)
FC2 (Fen)	No canopy	*Oxyoccus microcarpus* (5%), *Galium trifidum* (5%), *Carex* spp. (40%)	*Aulacomnium palustre* (100%)
FC3 (Fen)	No canopy	*Calla palustris* (10%), *Carex* spp. (20%)	*Brachythecium rivulare* (90%), bare ground (10%)

(Rutter et al., 1973; Aylesworth et al., 1993). Both bogs and fens are seasonally frozen wetlands with the water table remaining near the ground surface throughout the year. The bog surface is covered by *Sphagnum fuscum* and *Pleurozium schreberi*. Ericaceous shrubs, such as leatherleaf (*Chamaedaphne calyculata*), bog birch (*Betula glandulosa*), and northern bog-laurel (*Kalmia polifolia*), grow on slightly raised hummocks. The bog has a few stunted and scattered black spruce and tamarack (*Larix laricina*), and is surrounded on three sides by permafrost plateaus. The fen is a large linear feature which conveys water received from surrounding permafrost plateaus to the basin outlet (Quinton et al., 2003). The fen surface is covered by a buoyant *Sphagnum riparium*–dominated peat mat, which is approximately 0.5 to 1.0 m thick. The peat mat responds to changes in water table height, resulting in a variable surface elevation. The mat, which sits just below the water surface, supports the development of sedges, feather mosses, grasses, and various herbs and shrubs. The establishment of trees is minimal due to ground surface instability. Beneath the peat mat ($\sim$3 m) lies a dense organic layer with mineral soils (Hayashi et al., 2004).

Mean annual air temperature and precipitation measured at Fort Simpson is $-3.2\,°C$ and 369 mm, respectively. Approximately $\sim$46% of total precipitation falls as snow (from 1971 to 2000; MSC, 2002). The year studied (2008) was cooler with more snow than normal. Average annual air temperature was $-4.1\,°C$, and $\sim$72% of the cumulative precipitation for that year (361 mm) fell as snow. In 2008, snowmelt began in late March and ended during the first week of May.

Materials and Methods

CO$_2$ FLUXES

CO$_2$ fluxes were measured each day between 10:00 and 17:00 (CST) from 26 April to 6 June 2008 using a closed chamber system, which measured all fluxes within the chamber (c.f. Solondz et al., 2008; Petrone et al., 2011). This resulted in 44 measurements per chamber site throughout the spring snowmelt and the early plant growth (''green-up'') period (Fig. 1). Total respiration (R$_{tot}$) and net ecosystem exchange (NEE) from the soil and ground cover plants within the chamber were measured using the Vaisala CAR-BOCAP® GMP343 single-beam, dual-wavelength, nondispersive infrared Carbon Dioxide Probe (Vaisala Oyj, Vantaa, Finland). Terminology for NEE and R$_{tot}$ refers to within-chamber fluxes and does not extend to the ecosystem (as is the case with tower-based eddy covariance methods). The probe was inserted into the side of the chamber at a height of approximately half the height of the chamber. Clear polyvinylchloride (PVC) collars (interior radius = 12.3 cm, 40 cm tall) were inserted into the moss at each location on 12 April, two weeks prior to sampling (to minimize disturbance) and remained permanently in place for the duration of the study. As soils thawed, collars were cut deeper into the moss to a depth of 20 cm, while making note of headspace. This minimized damage to within chamber vegetation. NEE was measured within clear Lexan chambers, whereas R$_{tot}$ was measured during darkened conditions within a few minutes of NEE measurements after a two-layer opaque shroud was placed over the chamber system. The enclosed surface area of the tubular chamber was 0.56 m^2, with a volume of 0.03 m^3. Grooves were cut along the top of each collar and were filled with water before the chamber was placed on top of the collar. This ensured an airtight seal, limiting interaction be-

tween the chamber environment and the surrounding (outside) atmosphere. The interior air temperature was cooled by a flexible tube that was used to circulate water, thereby maintaining an interior chamber atmosphere within $\pm$2% of ambient air temperature (Petrone et al., 2011). A small fan mounted to the inside of the chamber at a height of approximately two-thirds the height of the chamber was used to circulate air for equilibration of gas concentrations and to avoid an artificial decrease in atmospheric gradient. During each chamber measurement CO$_2$ concentrations were measured every 30 s for a 5 min period (Table 2), and CO$_2$ flux was calculated as:

$$F = \frac{\Delta \cdot M}{N} \cdot \frac{V}{A} \tag{1}$$

where F is the gas flux (mg CO$_2$ m^2 s^{-1}), Δ is the linear change in CO$_2$ concentration with time (mg s^{-1}), M is the molar mass of CO$_2$ (44,010 mg mol^{-1}), N is the molar volume of a gas (0.224 m^3 mol^{-1}) at standard temperature and pressure (STP), V is the temperature corrected volume within the chamber (m^3) (using temperature measured on the GMP343 head), and A is the chamber area (m^2). To ensure the quality control of exchanges per chamber, each regression slope (change in CO$_2$ over the duration of each sampling interval, 30 s) was checked for significant deviation from a linear slope, and any measurements that were significantly different were removed, thereby removing any bias from the data set.

Timing of measurements per site were deliberately and randomly varied from day to day to minimize preferential sampling at specific hours within the day. A Kolmogorov-Smirnov (K-S) test used to determine if the timing of flux measurements throughout the day (e.g. biased grouping of measurements in the morning, late afternoon, etc.) varied significantly from one site to the next. The results indicate that the frequency and timing of data collection per site did not vary significantly ($p > 0.2$, in all cases), and therefore chamber data are comparable.

ENVIRONMENTAL MEASUREMENTS

Meteorology at Scotty Creek was described from measurements made at a meteorological tower located in the center of the bog, and detailed environmental measurements were made at each chamber location. These are described in Table 2.

Six representative soil cores (two from each site) were sampled near chamber locations at the end of the growing season (24 August 2008). Cores were inserted into the ground to a depth of 50 cm, and a depth of 20 cm was used (due to saturated conditions at bog/fen and compaction at plateau). Cores were cut horizontally into 5 cm subsamples, each with a volume of approximately 210 cm^3. Degree of decomposition (VonPost), total N (TN), total C (TC), and carbon-to-nitrogen (C:N) ratio of each subsample was determined. For C:N ratios, the samples were oven dried at 100 °C for 24 hours and ground in a tumbling ball mill for 2–5 min until homogenized into a powder for sampling. The percentage of TC and TN was determined through combustion utilizing an Isochrom–elemental analysis, Carlo–Erba Isotope Ratio Mass Spectrometry, autocombustion carbon–nitrogen analyzer (Micromass UK, Ltd., Environmental Isotope Laboratory, Department of Earth Sciences, University of Waterloo, Waterloo, Ontario, Canada).

TABLE 2

Daily and instantaneous measurements of flux and hydrometeorology at ecosystem level and at each individual chamber.

Location	Meteorological measurements (acronym) (units)	Sensor used	Instrument setup
Bog Tower	Air Temperature (Tair) (°C) & Relative Humidity (RH) (%)	HMP45C, Vaisala, Finland	2 m above the ground surface, 30-min average
	Precipitation (P) (rain) (mm)	Tipping bucket rain gauge (Jarek Manufacturing Ltd., Canada, calibrated to 0.25 mm per tip).	30-min cumulative P
Chamber Sites (internal chamber)	Tair (°C), RH (%)	Veriteq Spectrum SP-2000-20R data logger (Veriteq Instruments Inc., Canada)	0.25 m above ground surface, 1 s
Chamber Sites (external next/ near to chamber)	Photosynthetically active radiation (PAR) (Wm^{-2})	Quantum Meter	PAR level on top of chamber, measured simultaneously with flux measurements.
	Soil temperature (T$_{soil}$) (°C)	Digi-Sense Thermocouple, Type T, Model 60010-20, Eutech Instruments, Netherlands.	6 locations (measured at 0.1 m) at equal distances around inside edge of chamber collar at all sites
	Volumetric moisture content (VMC)	Hydrosense CD620, Campbell Scientific, Canada	Vertical measurements to 0.2 m
	Snow depth	Metric ruler	Within 1 m of chamber (but at distance so as not to be influenced by chamber), same location each time.
	Depth to frost table	1.2 m graduated steel rod	At location of snow depth, rod pushed into ground until depth of first refusal. Depths > 1.2 m were not measured.
	Water table depth	N/A	Cut away of rectangular section at soil depths of ~1cm until soil became saturated. Located 0.25 m from collar wall

AIRBORNE LIDAR ANALYSIS OF LOCAL TOPOGRAPHIC VARIABILITY AND SITE REPRESENTATION

Local topographic variability surrounding CO_2 measurement chambers was determined from airborne LiDAR data collected on 6 August 2008 (Chasmer et al., 2011b). Laser pulse reflections from the ground surface were classified into 'ground' returns in TerraScan software (Terrasolid, Finland). Returns within a 5 m radius of the chamber location were used to create a digital elevation model (DEM) at a resolution of 0.5 m based on an inverse distance weighting algorithm (O'Sullivan and Unwin, 2003) in Surfer (Golden Software, Inc., Colorado). An *x,y* search radius of 1 m and a power of one was used so that the return integrity (and ground surface morphology from a number of points) was maintained. The representation of chamber sites within the wider study area was also determined by applying a Boolean classification to ±1 standard deviation of topographic attributes (slope, aspect, highs, lows), and vegetation attributes (vegetation height and vegetation fractional cover) within a 2 m radius of each chamber site.

STATISTICAL ANALYSIS

Quantification of differences in measured CO_2 fluxes within and between land cover types, assuming that replication exists between all chambers per land cover type, was tested using Friedman repeated measures Analysis of Variance (RM ANOVA) on ranks where fluxes are not normally distributed at $P < 0.05$. Where they are normally distributed, a one-way RM ANOVA (with Chi-square test) is used instead. A time series analysis of land cover differences in NEE and R$_{tot}$ was also performed based on the differences between plateau vs. bog, plateau vs. fen, and bog vs. fen land cover types. The purpose was to quantify days when fluxes between land cover types were significantly different. Those days where land cover differences in average flux exceeded twice the standard deviation (approximately 95% confidence level) of the maximum land cover variance in NEE or R$_{tot}$ were considered significantly different. Multiple linear regression with an ordinary least squares estimation was used to determine correlation between multiple environmental controls on CO_2 fluxes. Relationships between fluxes and flux controlling mechanisms were determined using coefficient of determination (R^2) adjusted for covariance between controls. In all tests, a significance level of 0.05 (α) is used. Here we assume that chambers are representative of processes occurring at plateau, fen, and bog sites, but in reality, we cannot truly represent flux variability at the same land covers throughout the basin because of limited numbers of chambers. Therefore, caution is required when interpreting results.

Results

VARIABILITY OF AVERAGE CO₂ EXCHANGE BETWEEN LAND COVER TYPES

Average midday NEE at the bog, plateau, and fen chamber sites were 0.034 ± 0.025, 0.019 ± 0.013, and 0.014 ± 0.016 mg CO_2 m^{-2} s^{-1}, respectively, from 8 May to 6 June. A summary

TABLE 3

Average meteorological, hydrological, and fluxes of bog, fen, and plateau chamber sites. Numbers in parentheses represent ± 1 standard deviation. Incident PAR is at chamber height.

Site	T_{soil} (°C)	Volumetric Moisture Content (%)	Incident PAR (μmol m^{-2} s^{-1})	# Days where Frost Table Depth < 1 m	NEE (mg CO$_2$ m^2 s^{-1})	R_{tot} (mg CO$_2$ m^2 s^{-1})
PC1	1.96 (1.46)	27 (10.68)	835.88 (416.94)	>42	0.017 (0.012)	0.046 (0.024)
PC2	5.80 (3.43)	98 (2.44)	964.10 (460.32)	36	0.018 (0.022)	0.024 (0.026)
PC3	2.43 (1.8)	89 (10.94)	969.57 (453.07)	38	0.022 (0.016)	0.037 (0.021)
BC1	10.56 (5.42)	100 (0)	1026.92 (352.37)	12	0.016 (0.007)	0.020 (0.010)
BC2	9.76 (4.95)	100 (0)	1090.13 (427.07)	14	0.036 (0.02)	0.037 (0.019)
BC3	9.95 (5.01)	100 (0)	1116.66 (422.82)	12	0.055 (0.03)	0.052 (0.034)
FC1	11.43 (4.56)	100 (0)	1088.68 (328.0)	10	0.016 (0.016)	0.049 (0.027)
FC2	12.62 (4.67)	100 (0)	1179.1 (383.26)	12	0.007 (0.014)	0.035 (0.02)
FC3	10.63 (3.99)	100 (0)	1170.63 (437.75)	13	0.016 (0.021)	0.042 (0.016)

of fluxes and environmental conditions are presented in Table 3. Comparisons between chamber locations and land cover types based on one-way RM ANOVA indicate that there were no significant differences in NEE measured between plateau chambers (F = 2.5, p = 0.09, df = 2), but there were significant differences in NEE measured between fen chambers (RM ANOVA on ranks: Chi-square = 8.72, p = 0.013, df = 2) and bog chambers (RM ANOVA on ranks: Chi-square = 50.72, p < 0.001, df = 2). A time series analysis comparing daily average plateau, bog, and fen land cover types indicates that significant differences (p = 0.05) between plateau and bog average NEE occur only once during the entire time period examined, while significant differences between plateau and fen, and bog and fen occur on the first and last four to five days of the measurement period.

Average midday R_{tot} at bog, plateau, and fen chamber sites was 0.036 ± 0.026, 0.035 ± 0.026, and 0.042 ± 0.022 mg CO$_2$ m^{-2} s^{-1}, respectively. The bog was the greatest net source of CO$_2$ to the atmosphere (indicated by positive NEE and R_{tot}), ranging from 0.002 to 0.05 ± 0.02 mg CO$_2$ m^{-2} s^{-1}, despite greater R_{tot} from the fen, which was offset by uptake as the fen progressed from a source of CO$_2$ to a sink throughout the period studied (Fig. 2). As soils warmed in early June, R_{tot} at the plateau site increased rapidly from 0.03 to 0.09 ± 0.02 mg CO$_2$ m^{-2} s^{-1} over an 8-day period. R_{tot} was significantly different between chambers within land cover types (Chi-square = 24.261 [plateau]; 13.04 [bog]; and 28.58 [fen], p < 0.001, df = 2), and increases in site average PAR corresponded with increases in average NEE and R_{tot} at plateau and bog sites (although average T_{soil} does not correspond with average incident PAR). Daily differences between average R_{tot}, depending on land cover type, occurred most frequently between plateau and bog, where 6 of 34 days were significantly different and between bog and fen sites where 8 of 27 days were significantly different. Greatest differences occurred at the end of the measurement period. Differences between plateau and fen land cover types were not significant.

ENVIRONMENTAL CONDITIONS AND INFLUENCE ON CO$_2$ FLUXES

CO$_2$ fluxes were strongly influenced by the timing of snowmelt (Fig. 3). Average snow cover at the bog and fen sites persisted until DOY 121 (30 April) and 123 (2 May), respectively, and until DOY 126 (5 May) at the plateau sites. Deeper snowpack found at the plateau sites (45% greater than fen and bog) was caused by wind-driven drift and entrapment of snow within trees, reduced sublimation, and lower melt rates. Average T_{soil} at the permafrost plateau remained near 0 °C due to shallow frost table depth, but by DOY 153 (2 June) frost table depth had expanded, corresponding with an increase in T_{soil} (r^2 = 0.39, p < 0.001). Average T_{air} and T_{soil} increased linearly from 0 °C to ~14 °C (varying slightly per day). During the snow-cover period, fluxes remained below 0.02 (average = 0.015 ± 0.018) mg CO$_2$ m^{-2} s^{-1} at all sites, and were dominated by R_{tot}.

Increased rates of CO$_2$ flux into the atmosphere began on DOY 124 (3 May), increasing from 0.008 to 0.04 mg CO$_2$ m^{-2} s^{-1} one day after the snow pack disappeared at the bog site (on average for sites, including five days prior to and following snow disappearance). R_{tot} at the plateau sites increased starting on DOY 128 (7 May) (from 0.01 to 0.03 mg CO$_2$ m^{-2} s^{-1} on average), approximately two days following snow-free conditions. By DOY 128, CO$_2$ uptake increased at both the fen and permafrost plateau sites, while they both remained small net sources (Figure 2) (0.02 and 0.03 mg CO$_2$ m^{-2} s^{-1}, respectively).

Of the environmental drivers for CO$_2$ flux examined (including T_{soil}, depth to water table, PAR, and the number of days where the depth to the frost table was less than 1 m), daily average T_{soil} most strongly contributed to variability in R_{tot} and NEE at bog and fen sites, and depth to water table most strongly contributed to R_{tot} and NEE variability at plateau sites (Tables 4 and 5). PAR was a secondary driving mechanism of R_{tot} and NEE at all sites except at Fen chamber site 1 (FC1) (Tables 4 and 5) due to a mismatch in temporal scales between rapid variations in PAR and slower response to soil heating, ground thaw, microbial activity, and CO$_2$ exchanges. Fen and bog sites were saturated with water such that the water table rose above the ground surface. Therefore depth to water table was not included in this comparison at these sites.

MICROTOPOGRAPHIC INFLUENCES ON FLUXES

Topographic position of chamber sites did not necessarily influence ground vegetation species cover. Two plateau sites (PC1 and PC2) were dominated by *Sphagnum*, while PC3 contained
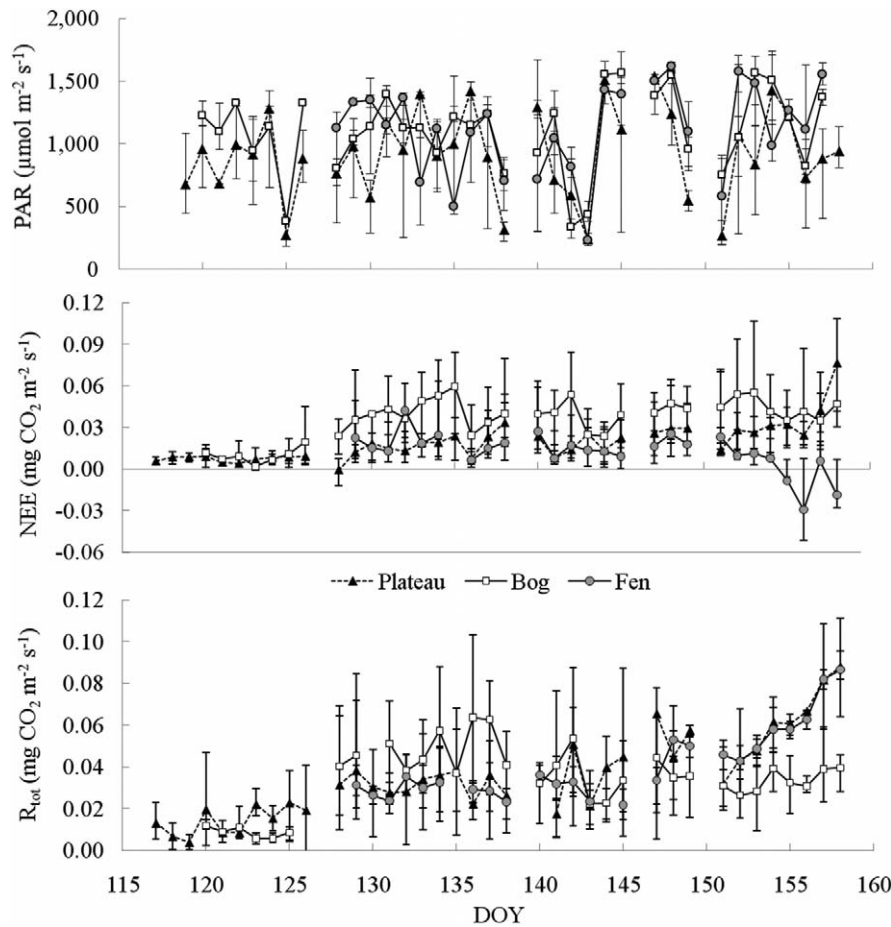
FIGURE 2. Daily average variability of photosynthetically active radiation (PAR) and CO_2 fluxes (NEE [net ecosystem CO_2 exchange] and R_{tot} [total respiration]) measured at three locations within plateau, bog, and fen land cover types. Bars represent maximum and minimum measured flux per land cover type. Incident PAR is highly variable due to local vegetation/cloud cover shadows.

mostly *Cladina rangiferina* (reindeer lichen). Significant differences in R_{tot} between chambers were found at plateau sites (discussed above). PC1 and PC3 were located within depressions of up to 1.5 m deep within a 5 m radius of the site location, while PC2 was located approximately near the middle of a 2.3° west-

facing slope (Fig. 4). Aboveground foliage cover was greater at PC1 and PC2 than at PC3 (Table 1), resulting in greater PAR incident at the ground surface at PC3. Soil and ground cover efflux were greatest at PC1 and PC3, corresponding with topographic depression and surprisingly lower average soil VMC at these sites.
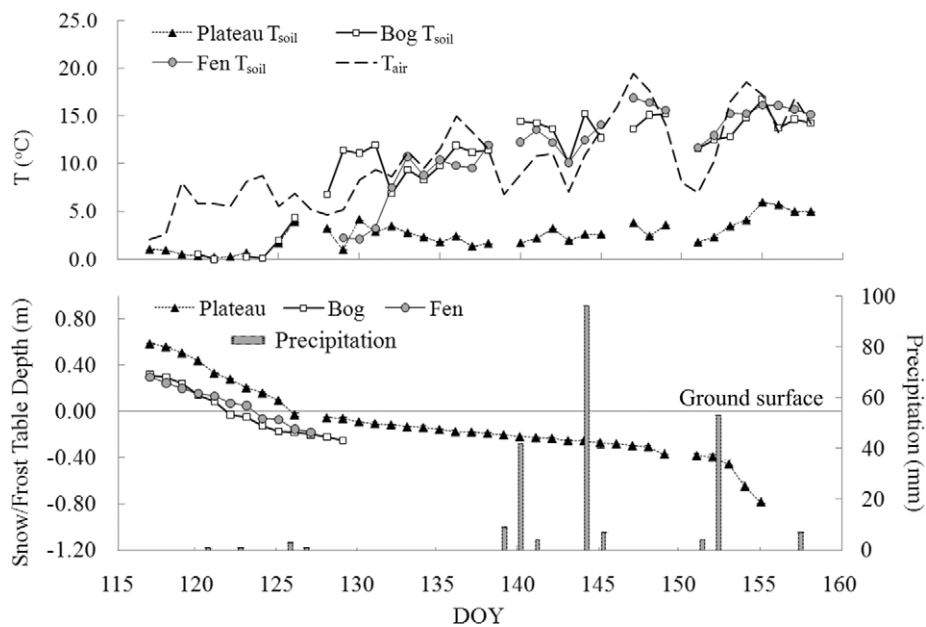

FIGURE 3. Average meteorological (T_{air} and T_{soil}) and hydrological (P, depth to frost table, and snow depth) measurements collected at plateau, bog, and fen chamber sites. T_{air} and P were measured at the bog meteorological tower. Snow depth and depth to frost table measurements are represented by the same symbols per site, where frost table begins at the ground surface (0 depth) following snowmelt. T_{soil} was measured at a depth of 0.1 m.

Explanation of variance in R_{tot} determined from multiple linear regression based on least squares method at plateau (PC), bog (BC), and fen (FC) sites. Contributions to variance are listed in order of importance (1 = more important, 2 = less important).

Site	Adjusted r^2 (p)	Contribution to variance 1 (Pearson's r)	Contribution to variance 2 (Pearson's r)
R_{tot} PC1	0.09 (0.42)	−0.30 (WT)	−0.06 (PAR)
R_{tot} PC2	0.66 (<0.05)	−0.83 (WT)	0.12 (PAR)
R_{tot} PC3	0.61 (<0.05)	−0.80 (WT)	0.46 (PAR)
R_{tot} BC1	0.05 (0.17)	0.32 (T_{soil})	−0.05 (PAR)
R_{tot} BC2	0.39 (<0.005)	0.65 (T_{soil})	−0.18 (PAR)
R_{tot} BC3	0.06 (0.14)	0.36 (T_{soil})	−0.03 (PAR)
R_{tot} FC1	0.32 (<0.05)	0.58 (T_{soil})	0.21 (PAR)
R_{tot} FC2	0.53 (<0.05)	0.69 (T_{soil})	0.48 (PAR)
R_{tot} FC3	0.14 (0.07)	0.39 (T_{soil})	0.22 (PAR)

Earlier active layer thaw and exposure of belowground biomass to oxygen at PC1 and PC3 likely dominated differences in R_{tot} compared with PC2, where active layer remained near the soil surface for a longer period of time.

All three bog sites were dominated by equal proportions of *Sphagnum capillifolium* and *S. fuscum.* Similarity in vegetation ground cover and minimal range of topographic variability at these sites (maximum 40 cm) makes it difficult to link CO_2 fluxes to topographic or vegetation communities. Yet significant differences in NEE and R_{tot} were found between sites (discussed above). BC1 had the lowest average NEE and R_{tot} and was dominated by an overstory of *Carex* spp., *Andromeda polifolia*, and *Chamaedaphne calyculata.* Increased overstory (sedge and shrub) species may have formed on this slightly sloped (0.06°, east-facing) surface (Fig. 4); however, these have not resulted in lower average T_{soil} compared with other sites (Table 3). In this case, higher average site T_{soil} was not related to greater CO_2 flux.

Significant differences in both NEE and R_{tot} were found at fen chamber sites using RM ANOVA (discussed above); however, differences in topographic variability were minimal (maximum range ~25 cm, and 5 cm within 1 m of chamber locations). Each site was located near the apex of the slope of small upraised areas within less than a meter from the chamber site location (Fig. 4). Average NEE was the same at FC1 and FC3, whilst average NEE and R_{tot} were less at FC2. Average T_{soil} was greatest at FC2 (Table 3), which was dominated by *Aulacomnium palustre* (bog moss), while FC1 and FC3 were dominated by feather moss and bry-

ophytes. Understory species coverage at FC2 was greater than the other two sites, but also had greatest average T_{soil} and incident PAR.

SOIL CHARACTERISTICS

C:N followed trophic differences between sites where highest C:N was found at the plateau and lowest at the channel fen (e.g. Trumbore et al., 1999). The ratio of C:N within the soil may also be used as an indicator of substrate quality, which may affect soil respiration through soil microbial activity. High N is often related to greater rates of decomposition of organic matter and higher rates of respiration (Raich and Schlesinger, 1992; Moore et al., 1998). R_{tot} was greatest at the plateau sites (average = 0.042 ± 0.02 mg CO_2 m^{-2} s^{-1}), despite a relatively high soil C:N of 55.9, low N (0.80%) (compared with fen and bog sites), and low VonPost humification scale (H1 to H3). Average R_{tot} at the fen site was slightly less than that measured at the plateau (0.041 ± 0.02 mg CO_2 m^{-2} s^{-1}), despite high total N (1.2%) and low C:N ratio (40.6) measured within the top 0.2 m of the soil column (Bekku et al., 2003). Further, porous and drier soils found at the plateau site (porosity average = 80.6% ± 4.1% within the upper 0.5 m) likely aided in movement and diffusion of CO_2 to the atmosphere.

Discussion

To date, variability of CO_2 fluxes between land cover types within northern discontinuous permafrost ecosystems is not well

TABLE 5

Explanation of variance in NEE (from multiple linear regression) at plateau (PC), bog (BC), and fen (FC) sites. Contributions to variance are listed in order of importance (1 = most important, 2 = less important, 3 = least important). NA = not applicable.

| Site	Adjusted r^2 (p)	Contribution to variance 1 (Pearson's r)	Contribution to variance 2 (Pearson's r)	Contribution to variance 3 (Pearson's r)
NEE PC1	0.42 (<0.05)	0.64 (T_{air})	−0.58 (PAR)	−0.08 (WT)
NEE PC2	0.31 (<0.05)	−0.53 (WT)	−0.26 (PAR)	−0.002 (T_{air})
NEE PC3	0.35 (<0.05)	−0.49 (WT)	0.33 (PAR)	0.02 (T_{air})
NEE BC1	0.11 (0.09)	0.34 (T_{soil})	0.19 (PAR)	NA
NEE BC2	0.28 (0.02)	0.57 (T_{soil})	−0.15 (PAR)	NA
NEE BC3	0.43 (<0.05)	0.68 (T_{soil})	−0.21 (PAR)	NA
NEE FC1	0.007 (0.36)	0.27 (PAR)	0.16 (T_{soil})	NA
NEE FC2	0.02 (0.30)	−0.27 (T_{soil})	−0.11 (PAR)	NA
NEE FC3	0.25 (0.02)	−0.46 (T_{soil})	−0.33 (PAR)	NA
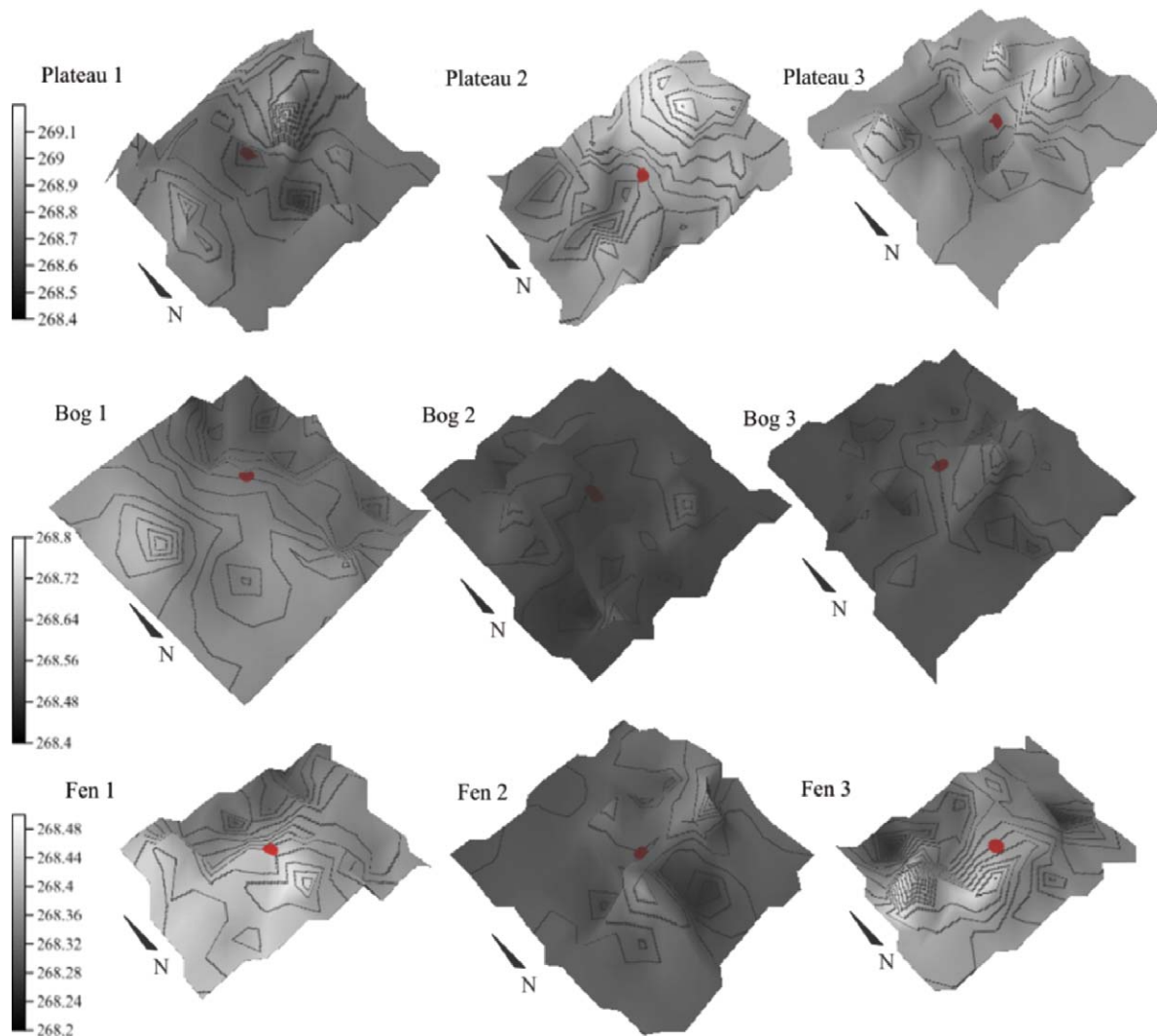
FIGURE 4. Microtopography characteristics within approximately 10 m × 10 m area surrounding chamber sites (red circle). Contour lines at 0.2 m height intervals are also shown. Area sizes vary slightly due to variable spacing of LiDAR returns.

understood. Highly variable microtopographical controls on soil moisture, soil temperature, and plant functional types can have significant influences on soil and ground cover CO_2 fluxes. At Scotty Creek, soil and ground cover fluxes were strongly related to soil moisture, soil temperature and the position of the frost table within the soil profile at daily time scales. Wright et al. (2009) found that depth to frost table on permafrost plateaus is highly variable over short distances of up to 1 m, and is strongly correlated to soil moisture distribution and lateral flow into subsurface depressions. When the soils are frozen, permafrost limits groundwater flow and storage capacity and decreases hydraulic conductivity (Wright et al., 2009). As soils thaw, the frost table and the water-saturated zone above it descends down through the soil profile, reducing saturated hydraulic conductivity and lateral flow (Quinton et al., 2000).

Topographical variability over very small distances also can have significant influences on plant functional types, which can alter the C sequestration potential of land cover types over broad areas, although these may be confounded by soil moisture (Petrone et al., 2011). Within plateaus, Wright et al. (2009) found significant

correlation between depth to frost table, soil moisture, and ground cover vegetation species at the same permafrost plateau examined in this study. They found that spatial ground coverage of mosses vs. lichens affected soil temperature and the rate of soil thaw in spring. *Sphagnum* mosses are able to retain capillary water far above the water table due to storage capacity of hyaline cells (Vitt, 2000; Lafleur et al., 2005), while lichens are not able to retain water, and act as thermal insulation by separating wet soil from the atmosphere (Rouse and Kershaw, 1971). Sulman et al. (2010) and Bubier et al. (1998) found that soil/ground cover efflux increased in topographically upraised areas within fens, whilst fluxes remained near zero in saturated hollows. The the opposite was true for bogs. Sulman et al. (2010) hypothesized that this may be related to the relative contributions of vascular and moss vegetation; where bogs contained mostly *Sphagnum* ground cover, fen sites contained more shrubs and sedges. They suggested that vascular species are more productive during dry periods, because they have greater maximum productivity than mosses and typically have higher GEP. This becomes more pronounced during drying periods. Petrone et al. (2011) found that *Sphagnum*-dominant lawns had the greatest

rate of uptake, while *Sphagnum*-dominant depressions, and feather moss-dominant depressions and lawns were net sources of CO_2. Differences in dominant plant functional types found among plateau, fen, and bog sites in the current study may also contribute to differences in fluxes, although linkages cannot be clearly defined (Table 3). Chamber sites contain up to 100% moss ground cover, while coverage of aboveground vascular species often varies among land cover types: up to 27% and 50% of chamber planar area contain vascular species (herbs and shrubs) within plateaus and fens, respectively, while vascular species are contained within up to 12% of the chamber planar area within bogs. Coverage of vascular vs. moss vegetation at fen and bog sites do not appear to influence NEE or R_{tot}; however, plateau and fen chamber sites containing increased coverage of vascular vegetation (PC1 and FC1) also have higher average R_{tot}. This may be due to litter production and decomposition from deciduous plants within the chamber, although the complexity of soil and vegetation interactions, microtopography, and biogeochemistry (e.g. losses due to dissolved organic C, methane, variability of soil nutrients, etc., not examined here) confound these results.

Microtopography may result in increased R_{tot} in areas between runoff channels, via aerobic conditions (Moore et al., 1998; Aerts et al., 2001; Bubier et al., 2003; Glenn et al., 2006). In this study, PC2 was located on a sloped surface and had the highest VMC compared with PC1 and PC2, which were located in slight depressions. Although the other two plateau chamber sites contributed more CO_2 to the atmosphere, on average, the proportion of R_{tot} to NEE was the lowest at this site. Chambers located at topographically high positions within the bog (e.g. BC1) released the lowest amount of CO_2 to the atmosphere, but in terms of the proportion of R_{tot} to NEE, respiration at this site was 20% greater than sequestration and was a much larger proportion of the flux than that measured at the other two (topographically lower) chamber sites. All chambers within the fen were located on a very slight slope, and therefore topographical influences were difficult to determine (although fluxes were significantly different at these sites). Petrone et al. (2011) found that differences in GEP were observed between *Sphagnum*-dominated lawns and depressions, while differences in GEP were not observed at feather moss sites of varying topographical elevation.

During the snowmelt period, fluxes remained below 0.02 (average = 0.015 ± 0.018) mg CO_2 m^{-2} s^{-1} at all sites (e.g. Zimov et al., 1996; Corradi et al., 2005; Elberling, 2007), and were dominated by R_{tot} due to limited photosynthesis by vegetation within chambers. A prolonged period of about 10 days of high R_{tot} is also found at the bog sites lagging the date of completely snow-free conditions and the start of frost table thaw by 2–3 days at plateau sites. This corresponds with an increase in air temperature from 8 °C to ~15 °C and warming soils (Fig. 3). CO_2 efflux continued at all flux sites throughout the period studied, except for the final four measurement days at the fen sites, where sites began to sequester CO_2. Photosynthesis resulted in a decrease in NEE at fen sites (Fig. 2), while NEE was relatively constant at bog and plateau sites (Griffis et al., 2000; Rouse et al., 2002). Low C:N ratio and greater productivity in the form of vigorous shrub development within the fen were evidence of increased nutrient availability due to plateau runoff and the movement of water through the channel fen

(NWWG, 1988). At fen chamber sites, increased vegetation production and growth correspond with greater rates of CO_2 sequestration (compared with bog and plateau). This resulted in higher maximum levels of gross ecosystem production (GEP), on average at fen sites (land cover average GEP peaked at 0.05 mg CO_2 m^{-2} s^{-1} [0.03 mg CO_2 m^{-2} s^{-1} on average throughout the measurement period]), than that for mosses, which are dominant in bogs (average landcover GEP = 0.0008 mg CO_2 m^{-2} s^{-1}). Further, mosses are more sensitive to water table height than vascular vegetation found within fens (e.g. Talbot et al., 2010). Average fluxes compare well with those of Myers-Smith et al. (2007), who used a similar methodology and data set. They found that growing season average midday NEE was 0.06 (± 0.017) mg CO_2 m^{-2} s^{-1} along a transect containing a collapsed (previously burned) plateau, moat, and bog in Alaskan discontinuous permafrost.

AERIALLY WEIGHTING MIDDAY SPRING CO_2 FLUXES BASED ON LAND COVER CHANGE

Increases in annual average air temperature of 1.6 °C and a lengthening of the snow-free period by approximately 14 days over the past 40 years (linear regression, $p = 0.07$, measured at Fort Simpson, Meteorological Service of Canada) has resulted in dramatic permafrost degradation and an increase in peatland areas at Scotty Creek. For example, Quinton et al. (2011) have shown that plateau area has decreased by approximately 11% between 1970 and 2008, and bog and fen areas have increased by 8% and 3%, respectively. Land cover conversion alters C fluxes, hydrology, and vegetation type/characteristics. Further, localized snow distribution and freeze-thaw cycles vary the timing of microbial activity, respiration, and photosynthesis. Historic aerial photography and high resolution topographical data provides a context from which these results may be further examined.

At Scotty Creek, the ratio of upraised areas to depressions indicates that 77% of the total watershed plateau area was above the planar surface, whilst 23% fell below (from LiDAR data). Ratios within fen and bogs were 37% to 63% and 22% to 78% (upraised:depression), respectively. Saturated land surface depressions within plateaus collapse into small, isolated bogs (Trumbore et al., 1999) and within fen and bog land cover types, depressions are more prevalent. At plateau edges, perimeter to area ratios have increased linearly from 0.03 (1947) to 0.08 (2008) (Chasmer et al., 2011a), and the proportion of isolated bogs within permafrost plateaus is ~15% of the cumulative plateau area (in 2008). Bogs are the greatest source of CO_2 to the atmosphere during the spring snowmelt and early green-up period, and 73% of the degraded plateau area has been converted into either isolated or connected bogs.

If chamber measurements are scaled according to their classified areas in 1970, a decrease in plateau area has the potential to reduce CO_2 fluxes by 26% during spring snowmelt. Increased fen and bog areas may result in increased CO_2 emissions by ~9% and 23%, respectively (all else being equal to 2008, including timing of snowmelt and onset of photosynthesis). Large-scale conversion of land covers may increase CO_2 effluxes by 7% based on land cover conversion alone. However, these results must be viewed with caution because only one plateau, one bog, and one fen are measured. Replication of this experiment at other sites within the

basin is required to add greater certainty to these results. Further, because both the bog and fen areas were saturated with water at the time of study, the extrapolation procedure implies that all bogs and fens within the basin must be completely saturated (adding even more uncertainty). Finally, this does not include total ecosystem flux at plateau sites (due to exclusion of trees and shrubs), and within some areas containing shrubs at fen sites. The characteristics (vegetation and topographic) found within chambers represent characteristics found within other plateaus, bogs, and fens 53%, 72%, and 59% of the time within a broader area, although important plant functional types are not included in this classification.

Conclusions

During the snowmelt and early spring green-up period, midday CO_2 exchanges observed at plateau, fen, and bog sites suggest that the ombrotrophic flat bog was the greatest source of CO_2 to the atmosphere, followed by permafrost plateau and channel fen. Relationships between CO_2 fluxes and soil/ground cover warming and drying in topographically upraised areas vs. establishment of localized plant communities as a result of shifting soil moisture regimes within plateau, fen, and bog sites are not clear during the spring thaw period at Scotty Creek. Interacting environmental driving mechanisms of C flux, including soil temperature, soil moisture, and PAR are confounded by cryospheric processes, the longevity of the frost table at the surface and movement through the soil profile, snow depth, cover, and timing of complete melt. The spatial distribution of plant functional types and biological mechanisms used by individual species to retain water and process C add additional complexity. Finally, biogeochemical processes, including nutrient flows and DOC and CH_4 losses were not considered, but also likely contributed to spatial and temporal variability in C uptake and respiration. In this study, the complexity of interacting processes influencing CO_2 exchanges over varying temporal and spatial scales makes quantification of a single descriptive proxy for NEE or R_{tot} difficult. For example, the timing of complete snow melt was strongly related to CO_2 exchanges at all sites, lagging between one day (bog and fen sites) and two days (plateau sites), on average. At plateau and bog sites, springtime average soil warming as a result of increased air temperatures and PAR incident on the ground surface corresponded with increased NEE and R_{tot}. However, at daily time periods T_{soil} and R_{tot} were not related to PAR due in part to a mismatch in temporal scales between rapidly varying PAR and slower rates of soil thaw and soil heating. Unraveling end member sites that have contrasting environmental, cryospheric, biogeochemical, and ecological traits will improve understanding of within land cover drivers of CO_2 fluxes. This is especially important as permafrost plateaus become increasingly fragmented, forming connected bog depressions, and greater volumes of water are conveyed through fens as a result of permafrost thaw.

Acknowledgments

References Cited

Aerts, R., Wallen, B., Malmer, N., and de Caluwe, H., 2001: Nutritional constraints on *Sphagnum* growth and potential decay in northern peatlands. *Journal of Ecology*, 89(2): 292–299.

Ansimov, O., and Reneva, S., 1996: Permafrost and changing climate: the Russian perspective. *AMBIO*, 35(4): 169–175.

Aylesworth, J. M., and Kettles, I. M., 2000: Distribution of fen and bog in the Mackenzie Valley, 60°N. Natural Resources Canada, *Geological Survey of Canada Bulletin*, 547.

Aylesworth, J. M., Kettles, I. M., and Todd, B. J., 1993: Peatland distribution in the Fort Simpson area, Northwest Territories with a geophysical study of peatland-permafrost relationships at Antoine Lake. *Geological Survey of Canada* Paper, 93-1E: 141–148.

Bekku, Y. S., Nakatsubo, T., Kume, A., Adachi, M., and Koizumi, H., 2003: Effect of warming on the temperature dependence of soil respiration rate in arctic, temperate and tropical soils. *Applied Soil Ecology*, 22(3): 205–210.

Bubier, J. L., Crill, P. M., Moore, T. R., Savage, K., and Varner, R. K., 1998: Seasonal patterns and controls on net ecosystem CO_2 exchange in a boreal peatland complex. *Global Biogeochemical Cycles*, 12(4): 703–714.

Bubier, J., Crill, P., and Mosedale, A., 2002: Net ecosystem CO_2 exchange measured by autochambers during the snow-covered season at a temperate peatland. *Hydrological Processes*, 16: 3667–3682.

Bubier, J. L., Bhatia, G., Moore, T. R., Roulet, N. T., and Lafleur, P. M., 2003: Spatial and temporal variability in growing-season net ecosystem carbon dioxide exchange at a large peatland in Ontario, Canada. *Ecosystems*, 6(4): 353–367.

Bubier, J., Moore, T. R., and Bledzki, L. A., 2007: Effects of nutrient addition on vegetation and carbon cycling in an ombrotrophic bog. *Global Change Biology*, 13: 1168–1186.

Camill, P., 1999: Patterns of boreal permafrost peatland vegetation across environmental gradients sensitive to climate warming. *Canadian Journal of Botany*, 77: 721–773.

Camill, P., and Clark, J. S., 1998: Climate change disequilibrium of boreal permafrost peatlands caused by local processes. *The American Naturalist*, 151: 207–222.

Camill, P., Lynch, J. A., Clark, J. S., Adams, J. B., and Jordan, B., 2001: Changes in biomass, aboveground net primary production, and peat accumulation following permafrost thaw in the boreal peatlands of Manitoba, Canada. *Ecosystems*, 4: 461–475.

Chasmer, L., Hopkinson, C., and Quinton, W. L., 2011a: Quantifying errors in permafrost plateau change from optical data, Northwest Territories, Canada: 1947 to 2008. *Canadian Journal of Remote Sensing–CRSS Special Issue*, 36(2): S211–S223.

Chasmer, L., Quinton, W. L., Hopkinson, C., Petrone, R., and Whittington, P., 2011b: Three-dimensional vegetation canopy characteristics within the discontinuous permafrost zone, Northwest Territories, Canada. *Permafrost and Periglacial Processes*, 22: 199–213, http://dx.doi.org/10.1002/ppp.724.

Corradi, C., Kolle, O., Walter, K., Zimov, S. A., and Schulze, E. D., 2005: Carbon dioxide and methane exchange of a north-east Siberian tussock tundra. *Global Change Biology*, 11(11): 1910–1925.

Elberling, B., 2007: Annual soil CO_2 effluxes in the High Arctic: the role of snow thickness and vegetation type. *Soil Biology & Biochemistry*, 39(2): 646–654.

Glenn, A. J., Flanagan, L. B., Syed, K. H., and Carlson, P. J., 2006: Comparison of net ecosystem CO_2 exchange in two peatlands in western Canada with contrasting dominant vegetation, *Sphagnum* and *Carex. Agricultural and Forest Meteorology*, 140: 115–135.

Gorham, E., 1991: Northern peatlands: role in the carbon-cycle and probable responses to climatic warming. *Ecological Applications*, 1(2): 182–195.

Goulden, M. L., Wofsy, S. C., Harden, J. W., Trumbore, S. E., Crill, P. M., Gower, S. T., Fries, T., Daube, B. C., Fan, S.-M., Sutton, D. J., Bazzaz, A., and Munger, J. W., 1998: Sensitivity of boreal forest carbon balance to soil thaw. *Science*, 279(5348): 214–217.

Griffis, T. J, Rouse, W. R., and Waddington, J. M., 2000: Interannual variability of net ecosystem CO_2 exchange at a subarctic fen. *Global Biogeochemical Cycles*, 14(4): 1109–1121.

Hayashi, M., Quinton, W. L., Pietroniro, A., and Gibson, J. J., 2004: Hydrologic functions of wetlands in a discontinuous permafrost basin indicated by isotopic and chemical signatures. *Journal of Hydrology*, 296(1–4): 81–97.

Hayashi, M., Goeller, N., Quinton, W. L., and Wright, N., 2007: A simple heat-conduction method for simulating the frost-table depth in hydrological models. *Hydrological Processes*, 21(19): 2610–2622.

Humphreys, E. R., and Lafleur, P. M., 2011: Does earlier snowmelt lead to greater CO_2 sequestration in two low Arctic tundra ecosystems? *Geophysical Research Letters*, 38: L09703, http://dx.doi.org/1029/2011GL047339.

Johansson, T., Malmer, N., Crill, P. M., Friborg, T., Akerman, J. H., Mastepanov, M., and Christensen, T. R., 2006: Decadal vegetation changes in a northern peatland, greenhouse gas fluxes and net radiative forcing. *Global Change Biology*, 12: 2352–2369.

Lafleur, P. M., Hember, R. A., Admiral, S. W., and Roulet, N. T., 2005: Annual and seasonal variability in evapotranspiration and water table at a shrub-covered bog in southern Ontario, Canada, *Hydrological Processes*, 19: 3533–3550, http://dx.doi.org/10.1002/hyp.5842.

Moore, T. R., Roulet, N. T., and Waddington, J. M., 1998: Uncertainty in predicting the effect of climatic change on the carbon cycling of Canadian peatlands. *Climatic Change*, 40(2): 229–245.

MSC, 2002: Canadian Climate Normals or Averages 1971–2000. Environment Canada, http://www.climate.weatheroffice.gc.ca.

Myers-Smith, I. H., McGuire, A. D., Harden, J. W., and Chapin, F. S., III, 2007: Influence of disturbance on carbon exchange in a permafrost collapse and adjacent burned forest. *Journal of Geophysical Research*, 112: G04017, http://dx.doi.org/10.1029/2007JG000423.

Myers-Smith, I. A., Harden, J. W., Wilmking, M., Fuller, C. C., McGuire, A. D., and Chapin, F. S., III, 2008: Wetland succession in a permafrost collapse: interactions between fire and thermokarst. *Biogeosciences*, 5: 1273–1286.

NWWG [National Wetlands Working Group], 1988: *Wetlands of Canada*. Ecological Land Classification Series, No. 24. Ottawa, Ontario: Sustainable Development Branch, Environment Canada, and Montreal: Poly Science Publications.

Oechel, W., Cowles, S., Grulke, N., Hastings, S. J., Lawrence, B., Prudhomme, T., Riechers, G., Strain, B., Tissue, D., and Vourlitis, G., 1994: Transient nature of CO_2 fertilization in Arctic tundra. *Nature*, 371: 500–503.

Oechel, W. C., Vourlitis, G. L., Hastings, S. J., Zulueta, R. C., Hinzman, L., and Kane, D., 2000: Acclimation of ecosystem CO_2 exchange in the Alaskan Arctic in response to decadal climate warming. *Nature*, 406: 978–981.

O'Sullivan, D., and Unwin, D. J., 2003: *Geographic Information Analysis.* Hoboken, New Jersey: Wiley.

Petrone, R. M., Kaufman, S., Devito, K. J., Macrae, M. L., and Waddington, J. M., 2005: Effect of drought on greenhouse gas emissions from pond/peatland systems with contrasting hydrologic regimes, northern Alberta, Canada. *In* Heathwaite, L., Webb, B., Rosenberry, D., Weaver, D., and Hayashi, M. (eds.), *Dynamics and Biogeochemistry of River Corridors and Wetlands*. IAHS Publication 294: 10–18.

Petrone, R. M., Solondz, D. S., Macrae, M. L., Gignac, D., and Devito, K. J., 2011: Microtopographical and canopy cover controls on moss carbon dioxide exchange in a western boreal plain peatland. *Ecohydrology*, 4(1): 115–129.

Quinton, W. L., and Marsh, P., 1999: A conceptual framework for runoff generation in a permafrost environment. *Hydrological Processes*, 13: 2563–2581.

Quinton, W. L., Gray, D. M., and Marsh, P., 2000: Subsurface drainage from hummock covered hillslopes in the Arctic tundra. *Journal of Hydrology*, 237(1,2): 113–125.

Quinton, W. L., Hayashi, M., and Pietroniro, A., 2003: Connectivity and storage functions of channel fens and flat bogs in northern basins. *Hydrological Processes*, 17(18): 3665–3684.

Quinton, W. L., Hayashi, M., and Chasmer, L., 2009: Peatland hydrology of discontinuous permafrost in the Northwest Territories: overview and synthesis. *Canadian Water Resources Journal*, 34(4): 311–328.

Quinton, W. L., Hayashi, M., and Chasmer, L., 2011: Permafrost-thaw-induced land-cover change in the Canadian subarctic: implications for water resources. *Hydrological Processes, Scientific Briefing*, 25: 152–158.

Raich, J. W., and Schlesinger, W. H., 1992: The global carbon dioxide flux in soil respiration and its relationship to vegetation and climate. *Tellus*, 44(B2): 81–99.

Robinson, S. D., and Moore, T. R., 2000: The influence of permafrost and fire upon carbon accumulation in high boreal peatlands, Northwest Territories, Canada. *Arctic, Antarctic, and Alpine Research*, 32(2): 155–166.

Rouse, W. R., and Kershaw, K. A., 1971: The effects of burning on the heat and water regimes of lichen-dominated subarctic regimes. *Arctic and Alpine Research*, 3(4): 291–304, http://dx.doi.org/10.2307/1550045.

Rouse, W. R., Bello, R. L., D'Souza, A., Griffis, T. J., and Lafleur, P. M., 2002: The annual carbon budget for fen and forest in a wetland at Arctic treeline. *Arctic*, 55(3): 229–237.

Rutter, N. W., Boydell, A. N., Savigny, K. W., and van Everdingen, R. O., 1973: Terrain evaluation with respect to pipeline construction, Mackenzie pipeline construction: southern part lat. 60° to 64°N. Ottawa, Ontario: Environmental Soc. Comm. Northern Pipelines, Task Force on Northern Oil Development, Report No. 73–36, 135 pp.

Solondz, D. S., Petrone, R. M., and Devito, K., 2008: Forest floor carbon dioxide fluxes within an upland-peatland complex in the Western Boreal Plain, Canada. *Ecohydrology*, 1(4): 361–376.

Strack, M., Waddington, J. M., Rochefort, L., Tuittila, E. S., 2006: Responses of vegetation and net ecosystem carbon dioxide exchange at different peatland microforms following water table drawdown. *Global Biogeochemical Cycles*, 11: G02006, http://dx.doi.org/10.1029/2005JG000145.

Sulman, B. N., Desai, A. R., Saliendra, N. Z., Lafleur, P. M., Flanagan, L. B., Sonnentag, O., Mackay, D. S., Barr, A. G., and van der Kamp, G., 2010: CO_2 fluxes at northern fens and bogs have opposite responses to inter-annual fluctuations in water table. *Geophysical Research Letters*, 37: L19702, http://dx.doi.org/10.1029/2010GL044018.

Talbot, J., Richard, P. J. H., Roulet, N. T., and Booth, R. K., 2010: Assessing long-term hydrological and ecological responses to drainage in a raised bog using paleoecology and a hydrosequence. *Journal of Vegetation Science*, 21(1): 143–156, http://dx.doi.org/10.1111/j.654-1103.2009.01128.x.

Trumbore, S. E., Bubier, J., Harden, J., and Crill, P., 1999: Carbon cycling in boreal wetlands: a comparison of three approaches. *Journal of Geophysical Research*, 104(D22): 27673–27682.

Turetsky, M. R., Wieder, R. K., Williams, C. J., and Vitt, D. H., 2000: Organic matter accumulation, peat chemistry, and permafrost melting in peatlands of boreal Alberta. *Écoscience*, 7: 379–392.

Turetsky, M. R., Wieder, R. K., and Vitt, D. H., 2002: Boreal peatland C fluxes under varying permafrost regimes. *Soil Biology & Biochemistry*, 34: 907–912.

Vitt, D. H., 2000: Peatlands: ecosystems dominated by bryophytes. *In* Shaw, J. R., and Goffinet, B. (eds.), *Bryophyte Biology*. Cambridge, U.K.: Cambridge University Press, 312–343.

Waddington, J. M., and Roulet, N. T., 1996: Atmosphere-wetland carbon exchanges: scale dependency of CO_2 and CH_4 exchange on the developmental topography of a peatland. *Global Biogeochemical Cycles*, 10(2): 233–245.

Ward, S. E., Bardgett, R. D., McNamara, N. P., and Ostle, N. J., 2009: Plant functional group identity influences short-term peatland ecosystem carbon flux: evidence from a plant removal experiment. *Functional Ecology*, 23: 454–462.

Wilson, K. S., and Humphreys, E. R., 2010: Carbon dioxide and methane fluxes from Arctic mudboils. *Canadian Journal of Soil Science*, 90: 441–449.

Wright, N., Quinton, W. L., and Hayashi, M., 2008: Hillslope runoff from ice-cored peat plateaus in a discontinuous permafrost basin, Northwest Territories, Canada. *Hydrological Processes*, 22: 2816–2828.

Wright, N., Hayashi, M., and Quinton, W. L., 2009: Spatial and temporal variations in active layer thawing and their implication on runoff generation in peat-covered permafrost terrain. *Water Resources Research*, 45(5): W05414, 13 pp., http://dx.doi.org/10.1029/2008WR006880.

Zimov, S. A., Davidov, S. P., Voropaev, Y. V., and Prosiannikov, S. F., 1996: Siberian CO_2 efflux in winter as a CO_2 source and cause of seasonality in atmospheric CO_2. *Climatic Change*, 33: 111–120.